

**RL-TR-96-282**  
**Final Technical Report**  
**April 1997**



# **STUDIES OF A PHOTONIC DELAY LINE FOR APPLICATION TO FREQUENCY- AGILE, WIDEBAND RADAR SYSTEMS**

**LeMoyne College**

**Evelyn H. Monsay**

*APPROVED FOR PUBLIC RELEASE; DISTRIBUTION UNLIMITED.*


19970715 214

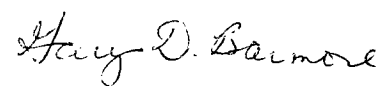
**DTIC QUALITY INSPECTED 4**

**Rome Laboratory**  
**Air Force Materiel Command**  
**Rome, New York**

This report has been reviewed by the Rome Laboratory Public Affairs Office (PA) and is releasable to the National Technical Information Service (NTIS). At NTIS it will be releasable to the general public, including foreign nations.

RL-TR-96-282 has been reviewed and is approved for publication.

APPROVED:   
PAUL M. PAYSON  
Project Engineer

FOR THE COMMANDER:   
GARY D. BARMORE, Major, USAF  
Deputy Director  
Surveillance & Photonics Directorate

If your address has changed or if you wish to be removed from the Rome Laboratory mailing list, or if the addressee is no longer employed by your organization, please notify RL/OCPC, 25 Electronic Pky, Rome, NY 13441-4514. This will assist us in maintaining a current mailing list.

Do not return copies of this report unless contractual obligations or notices on a specific document require that it be returned.

<b>REPORT DOCUMENTATION PAGE</b>			Form Approved OMB No. 0704-0188	
Public reporting burden for this collection of information is estimated to average 1 hour per response, including the time for reviewing instructions, searching existing data sources, gathering and maintaining the data needed, and completing and reviewing the collection of information. Send comments regarding this burden estimate or any other aspect of this collection of information, including suggestions for reducing this burden, to Washington Headquarters Services, Directorate for Information Operations and Reports, 1215 Jefferson Davis Highway, Suite 1204, Arlington, VA 22202-4302, and to the Office of Management and Budget, Paperwork Reduction Project (0704-0188), Washington, DC 20503.				
1. AGENCY USE ONLY (Leave blank)		2. REPORT DATE April 1997	3. REPORT TYPE AND DATES COVERED FINAL, Jul 94 - Jul 95	
4. TITLE AND SUBTITLE <b>STUDIES OF A PHOTONIC DELAY LINE FOR APPLICATION TO FREQUENCY-AGILE, WIDEBAND RADAR SYSTEMS</b>			5. FUNDING NUMBERS C - F30602-94-C-0234 PE - 62702F PR - 4600 TA - P2 WU - PS	
6. AUTHOR(S) Evelyn H. Monsay				
7. PERFORMING ORGANIZATION NAME(S) AND ADDRESS(ES) LeMoyne College 1419 Salt Springs Rd. Syracuse NY 13214			8. PERFORMING ORGANIZATION REPORT NUMBER  N/A	
9. SPONSORING / MONITORING AGENCY NAME(S) AND ADDRESS(ES) Rome Laboratory/OCPC 25 Electronic Pky Rome NY 13441-4515			10. SPONSORING / MONITORING AGENCY REPORT NUMBER  RL-TR-96-282	
11. SUPPLEMENTARY NOTES  Rome Laboratory Project Engineer: Paul M. Payson, OCPC, (315) 330-7911				
12a. DISTRIBUTION AVAILABILITY STATEMENT  Approved for Public Release; Distribution Unlimited			12b. DISTRIBUTION CODE	
13. ABSTRACT (Maximum 200 words) A method is described by which adaptive beamforming can be accomplished in transmit mode with a photonic true time delay beamformer. Performance predictions for a radar line array using this beamformer are also presented. Possible configurations for a photonic true time delay beamformer in the receive mode are also discussed. Particular attention is paid to the possibilities for broadband/frequency agile closed-loop adaptive beamforming using a photonic receiver.				
14. SUBJECT TERMS phased arrays, optical heterodyning, photonic delay line, adaptive beamforming			15. NUMBER OF PAGES 36	
			16. PRICE CODE	
17. SECURITY CLASSIFICATION OF REPORT UNCLASSIFIED	18. SECURITY CLASSIFICATION OF THIS PAGE UNCLASSIFIED	19. SECURITY CLASSIFICATION OF ABSTRACT UNCLASSIFIED	20. LIMITATION OF ABSTRACT UNLIMITED	

# ADAPTIVE BEAMFORMING WITH A PHOTONIC DELAY LINE

## ABSTRACT

A method is described by which adaptive beamforming can be accomplished in transmit mode with a photonic true time delay beamformer. Performance predictions for a radar line array using this beamformer are also presented.

Possible configurations for a photonic true time delay beamformer in the receive mode are also discussed. Particular attention is paid to the possibilities for broadband/frequency agile closed-loop adaptive beamforming using a photonic receiver.

ADAPTIVE BEAMFORMING WITH A  
PHOTONIC DELAY LINE

TABLE OF CONTENTS

<u>SECTION</u>	<u>PAGE</u>
1. INTRODUCTION - TRANSMIT MODE	1
2. STANDARD BEAMFORMING WITH THE PHOTONIC TRUE TIME DELAY LINE	2
3. METHOD FOR ADAPTIVE BEAMFORMING	5
4. RESULTS - TRANSMIT MODE	7
5. DISCUSSION - TRANSMIT MODE	11
6. INTRODUCTION - RECEIVE MODE	12
7. CONFIGURATION FOR A BROADBAND RECEIVER	14
8. ADAPTIVE CONFIGURATIONS OF THE PHOTONIC RECEIVER	16
A. CONFIGURATION USING THE SMD	16
B. TOTALLY PHOTONIC CONFIGURATIONS OF A FULLY ADAPTIVE BEAMFORMER	17
C. A FULLY ADAPTIVE EXTENSION OF THE TOUGHLIAN/ ZMUDA RECEIVE BEAMFORMER	20
9. DISCUSSION - RECEIVE MODE	20
10. REFERENCES	22

## LIST OF FIGURES

### PAGE

- |    |              |  |
|----|--------------|--|
| 4  | Figure 1(a): | Beampattern of a conventional true time delay (TTD) beamformer for a 10-element line array, steered to $0^\circ$ .   |
| 4  | Figure 1(b): | Beampattern of a conventional photonic beamformer for a 10-element line array, steered to $0^\circ$ .  |
| 9  | Figure 2(a): | Beampattern of an adaptive true time delay (TTD) beamformer for a 10-element line array, steered to $0^\circ$ , with "jammer" at $20^\circ$ and null steered to $20^\circ$ . |
| 9  | Figure 2(b): | Beampattern of an adaptive photonic beamformer for a 10-element line array, steered to $0^\circ$ , with "jammer" at $20^\circ$ and null steered to $20^\circ$ .              |
| 10 | Figure 3(a): | Beampattern of an adaptive true time delay (TTD) beamformer for a 10-element line array, steered to $0^\circ$ , with "jammer" at $40^\circ$ and null steered to $40^\circ$ . |
| 10 | Figure 3(b): | Beampattern of an adaptive photonic beamformer for a 10-element line array, steered to $0^\circ$ , with "jammer" at $40^\circ$ and null steered to $40^\circ$ .              |
| 15 | Figure 4:    | Single quantized variable delay line and experimental setup [15].  |
| 15 | Figure 5:    | Schematic diagram of the full Toughlian/Zmuda phased array receiver [15].  |
| 18 | Figure 6:    | Fully adaptive - spatially and spectrally - photonic receiver system [16].   |
| 18 | Figure 7(a): | Acousto-optic cell system for producing tap weights [21].  |
| 18 | Figure 7(b): | Optical system to produce Fourier transform of tap weights [21].   |
| 19 | Figure 8:    | Penn's adaptive interference canceller using time and space integrating correlators [22].  |
| 19 | Figure 9:    | Schematic diagram of a fully adaptive photonic receive beamformer.   |

## ADAPTIVE BEAMFORMING WITH A PHOTONIC DELAY LINE

### 1. INTRODUCTION - TRANSMIT MODE

A photonic true time delay beamformer has been previously introduced and studied<sup>1-2</sup> which relies on the optical read-out of the time delay along the acoustic wave in an acousto-optic modulator (AOM) in an optical heterodyne system for generating the correct phase shifts for elements in a radar array. Several experimental studies<sup>2-4</sup> have demonstrated the essential validity of this concept. An analytical understanding of the minor limitations of this concept has also been obtained<sup>5-8</sup>. To date, the photonic beamformer has been conceived of primarily in the transmit mode; major reconfiguration of the system is anticipated for operation as a receiver. Hence, this study of the use of the photonic true time delay line as an adaptive beamformer is also dedicated to the transmit mode of operation.

Adaptive beamforming in the transmit mode of operation should be viewed as transmitting energy so as to minimize unwanted reflections, a source of noise. For example, a null steering operation for a transmit array would seek to minimize the energy emitted in the direction of a known, unimportant scattering object. This function must rely on a priori knowledge of where the undesirable scatterers (such as buildings, trees, etc.) are. Note that in receive array adaptive filtering, a priori knowledge is also required, usually knowledge of the direction of arrival and spectrum of the desired signal(s)<sup>9,10</sup>.

In Section 2, a review of some of the results of performance predictions for standard beamforming using the photonic true time delay line is given. In standard beamforming, a single frequency signal focussed in a chosen direction is the goal, with pointing accuracy (no beam squint), array gain or directionality, and sidelobe level as the performance criteria. The photonic beamformer theoretically performs quite well in this role, with excellent support from experimental results already obtained.

In Section 3, the requirements for adaptive beamforming are discussed with respect to the capabilities of the photonic true time delay line. A method for using the photonic delay line as an adaptive beamformer is described, and justification for the validity of this extension of the original concept is given. Potential limitations are described and evaluated.

In Section 4, the results of simulated beampatterns for adaptive transmit beamforming using the photonic true time delay line, based on the method described in Section 3, are presented and evaluated. Finally, in Section 5, conclusions as to the potential for adaptive beamforming, in the transmit mode, using

the photonic beamformer, are presented.

## 2. STANDARD BEAMFORMING WITH THE PHOTONIC TRUE TIME DELAY LINE

For an ideal true time delay beamformer, steered to angle  $\theta_o$  and scanned at an angle  $\theta_s$ , the beampattern is given by<sup>11,12</sup>

$$b(\theta_o, \theta_s, k) = \left| \sum_{n=1}^N \exp(j \frac{\omega d n}{c} (\sin \theta_o - \sin \theta_s)) \right|^2 \quad (1)$$

For the photonic beamformer under consideration here, the actual time delay between radar transmitters is incorporated into Equation (1) by recognizing that  $\omega d n / c$  can be replaced by the phase function  $\Phi(x, \omega)$ ,

$$\Phi(x, \omega) = \text{atan} \left[ \frac{\sin(\beta x) \int_{-\frac{1}{d_0} + \beta}^{\frac{1}{d_0} + \beta} \frac{\sin(au)}{u} \cos(xu) du - \cos(\beta x) \int_{-\frac{1}{d_0} + \beta}^{\frac{1}{d_0} + \beta} \frac{\sin(au)}{u} \sin(xu) du}{\sin(\beta x) \int_{-\frac{1}{d_0} + \beta}^{\frac{1}{d_0} + \beta} \frac{\sin(au)}{u} \sin(xu) du + \cos(\beta x) \int_{-\frac{1}{d_0} + \beta}^{\frac{1}{d_0} + \beta} \frac{\sin(au)}{u} \cos(xu) du} \right] \quad (2)$$

calculated for each specific transmitter  $n$ . In this equation,  $u = (k - \beta)$ , where  $k = 2\pi/\Lambda$  and  $\Lambda$  is the acoustic wavelength in the AOM. Also,  $\beta = \omega/v$ , where  $\omega$  is  $2\pi f$ , and  $v$  is the acoustic velocity in the AOM, and  $2a$  is the width of the illuminated region. The parameter  $d_0$  is given by  $(\lambda F)/d$ , where  $\lambda$  is the optical wavelength,  $F$  is the focal length of the lens which focuses the probe beam in the AOM, and  $d$  is the unfocussed beam diameter.

The beamwidth is typically defined as the spread of the main lobe of the beampattern, taken between angles at which the power in the pattern is reduced by 3dB. For the ideal conventional beamformer for a ten-element line array, the full beamwidth at half-maximum power (FWHM) is  $16.95^\circ$ , as determined from the calculations performed to obtain Figure 1a. For the photonic true time delay beamformer, as modeled in Equation (2), the FWHM is  $16.75^\circ$ , a value  $0.2^\circ$  ( $3.49 \times 10^{-3}$  radians) narrower than the



ideal conventional beamformer. This result is unexpected, and may be a fortuitous phase-related self-focusing due to the non-random nature of the diffraction-induced phase nonlinearities.

The manner in which most energy is lost out of the main beam is through projection in the directions of the next highest peaks in the beampattern - the primary sidelobes. The maximum primary sidelobe level for the ten-element line array, for the ideal conventional beamformer, is found to be 13dB down from the mainlobe peak level. The sidelobe reaches its peak value at 17°. Calculations for the same line array using the modeled photonic beamformer yield a peak primary sidelobe level 13.42dB down from the mainlobe peak, lower than the ideal conventional beamformer produces. Again, this very slight improvement over the conventional beamformer is unexpected and fortuitous; it may not hold for all array configurations of interest. However, there is certainly no degradation in the case of the modeled photonic beamformer. The sidelobe peak for the photonic beamformer is centered at 16°.

While the primary sidelobes are of greatest importance in terms of the control of noise and beamforming accuracy, unusually high secondary sidelobes may also be a cause for concern. As is evident from Figure 1b, the photonic beamformer has much higher sidelobes at 90° and 270° than the ideal true time delay (TTD) beamformer; whereas the TTD beamformer has nulls at these angles, the photonic beamformer has sidelobes at a level 22.22 dB down from the mainlobe. The explanation<sup>13</sup> for the higher-level secondary sidelobes in the photonic beamformer is that it is essentially a beam squint effect, even though the more usual beam squint effect on the mainbeam pointing direction does not appear.

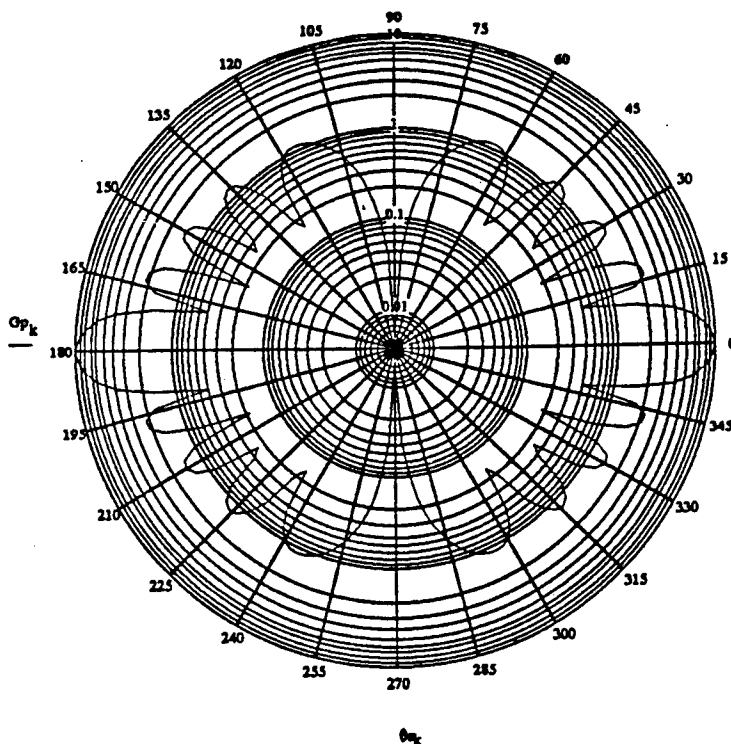
The array gain of a beamformer measures how well the antenna can concentrate energy in a particular direction, compared to an isotropic radiator. It is given by the ratio of the gain achieved in the detection of the coherent signal, over the gain provided by the multi-element array in the detection of the incoherent noise<sup>12</sup>. For an ideal conventional beamformer and a ten-element line array, the array gain is a factor of ten.

The signal gain for a general phased array is given by

$$g_s = \left| \sum_{n=0}^N e^{j\omega(\hat{\tau}_n - \tau_n)} \right|^2 = \left| \sum_{n=0}^N e^{j(\hat{\Phi}_n - \Phi_n)} \right|^2 \quad (3)$$

where, for the photonic beamformer,  $\hat{\tau}_n$  is the value provided for the n-th array element by Equation (2). The signal gain for a ten-element line array (N=10), based on the photonic beamformer, is calculated to be 89.375dB. For perfectly incoherent noise,

(a)



(b)

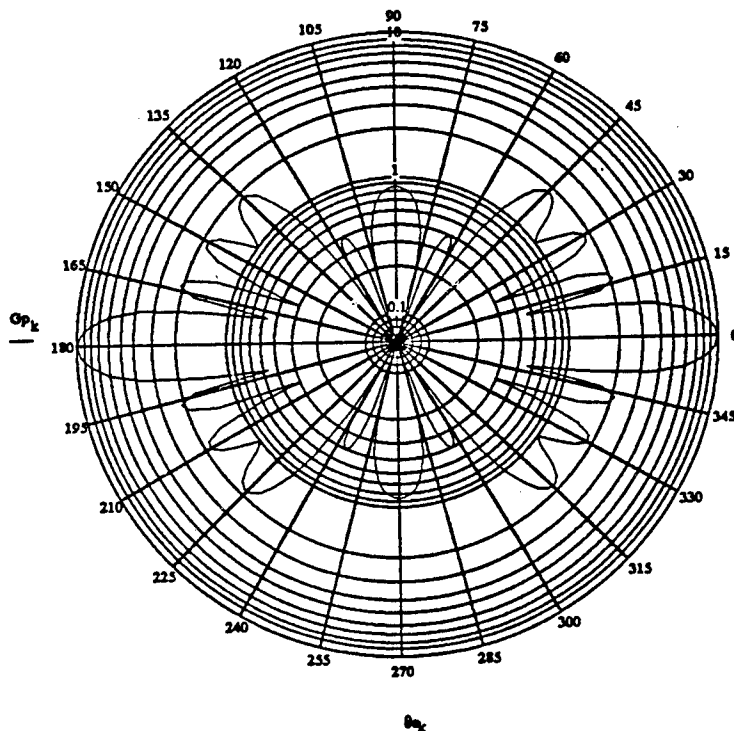


Figure 1: (a) Beampattern of a conventional true time delay (TTD) beamformer for a 10-element line array, steered to  $0^\circ$ ;  
(b) Beampattern of a conventional photonic beamformer for a 10-element line array, steered to  $0^\circ$ .

the noise gain is 10dB, and so the array gain is

$$\text{Array Gain (AG)} = \frac{G_s}{N} = 8.9375. \quad (4)$$

The array efficiency compares the array gain of the beamformer under investigation to that of the equivalent ideal conventional beamformer.

Hence,

$$\text{Array Efficiency} = \frac{AG}{10} = 0.89375, \quad (5)$$

so the photonic beamformer has an array efficiency of 89.375 percent.

### 3. METHOD FOR ADAPTIVE BEAMFORMING

In conventional beamforming, the acoustic wave in the AOM is used as an "analog computer" for the radar beam one wishes to form, in that its phase at the location of the reference beam, used as a "probe", automatically provides the correct phase shift to an analogous element in the radar array. In adaptive beamforming with the photonic true time delay line, the direct relationship between the acoustic wave in the AOM and the desired radar beam no longer holds, primarily for two reasons. First, both amplitude and phase (not just phase alone, as before) must be controlled for each radar element. Second, the phase shifts required by each radar element are no longer related to the natural phase shifts of a plane wave. So, a method must be devised by which the particular amplitude and phase for each radar element can be "read off" by a probe beam from the acoustic wave in an AOM, if the general concept of the photonic true time delay line is to be generalized for adaptive beamforming.

The approach taken here is to construct an appropriate multi-frequency RF time waveform based on independent, monochromatic waves of the required amplitudes and frequencies so that each radar element can be represented by just one such wave at a particular location in the AOM. The phase shift given to a particular radar element will depend on

$$\Phi_n = \frac{2\pi fx}{v} = \phi_n \quad (6)$$

where now  $\phi_n$  is the value of the phase shift of the n-th radar element as required by the adaptive beamforming algorithm, as will be discussed below. From Equation (6), it is apparent that either frequency,  $f$ , or AOM location,  $x$ , could be manipulated to get the desired phase shift. However, control over the amplitude

is also required for this element, so it is most useful to fix  $x$  and use a monochromatic wave with its frequency chosen to satisfy Equation (6), and with an amplitude that matches the amplitude also required by the adaptive algorithm.

The goal is to have a weight matrix  $W$  given in terms of the weight vector for steering in direction  $\theta_s$ ,  $W_q$ , beampattern factor  $G_q$ , and a vector  $B^q$ , where

$$B_t = [1, \exp(j\beta), \exp(j2\beta), \dots, \exp(j(K-1)\beta)] \quad (7)$$

$$(W_q)_t = [a_1, a_2 \exp(-j\beta_s), a_3 \exp(-j2\beta_s), \dots, a_K \exp(-j(K-1)\beta_s)] \quad (8)$$

$$G_q(\beta) = B_t W_q \quad (9)$$

with  $\beta = (2\pi d/\lambda) \sin \theta$ ,  $\beta_s = (2\pi d/\lambda) \sin \theta_s$ , the  $a_j$  are real amplitudes, and where a subscript  $t$  denotes the transpose of a vector. In terms of Equations (7) through (9),  $W$  is given by

$$W = W_q - G_q B \quad (10)$$

in the absence of noise. Then  $W = \{W_n\}$ , can be expressed as an amplitude and a phase for each element  $n$ , where

$$\phi_n = \text{atan} \left( \frac{\text{Im}(W_n)}{\text{Re}(W_n)} \right) \quad (11)$$

and

$$a_n = \sqrt{\text{Re}(W_n)^2 + \text{Im}(W_n)^2} \quad (12)$$

The  $\phi_n$  and  $a_n$  of Equations (11) and (12), respectively, give the required read-out phase and amplitude for radar element  $n$ . The frequency of each component wave of the RF input to the AOM will be given via Equation (6); the amplitude of each wave is directly given by Equation (12).

The new beampattern is given by

$$G(\beta) = B_t W_q - \left( \frac{1}{1+K} \right) G_q(\beta_j) B_t B_j^* \quad (13)$$

It is necessary to realize that the beampattern given by Equation

(13) is still complex in that form and one must take  $G_q(\beta) \cdot G_q(\beta)^*$  in order to get a real power beampattern (which will be equivalent to that obtained from Equation (1)).

In order to be able to incorporate the diffraction effects of the photonic beamformer in this more general, idealized set of equations, it is necessary to realize that

$$e^{jn\beta} = e^{j\hat{\Phi}_n \sin(\theta)} \quad (14)$$

In the next Section, results of using these formulas for a 10-element line array for both the TTD and photonic beamformers will be presented and discussed, as will the results of selection of a set of monochromatic waves to be input to the AOM which could generate the required weights,  $W_n$ .

#### 4. RESULTS - TRANSMIT MODE

Figures 1a and 1b presented the conventional beampatterns for the TTD and photonic beamformers, respectively. In Figures 2a and 2b, a very noisy "jammer" at  $20^\circ$  - actually, in our transmit case, we are referring to a very large signature, undesired reflector - has been nulled, to some extent, by the adaptive beamforming technique described in Section 3. While it is evident that the adaptive nulling is not optimized, it is also clear that the photonic beamformer does as well as the TTD beamformer in removing the effect of the "jammer". Figures 3a and 3b are beampatterns incorporating "jammers" at  $40^\circ$  and the adaptive null steering described before. Standard techniques of adaptive beamforming would be useful to enhance the basic results shown in these figures. Again, however, the important point here is that the photonic beamformer does as well as an ideal TTD beamformer.

Following the prescription embodied in Equations (6) and (11), as described in Section 3, the required monochromatic waves which must be added and sent into the AOM as the RF input are described by the frequencies found in Table 1.

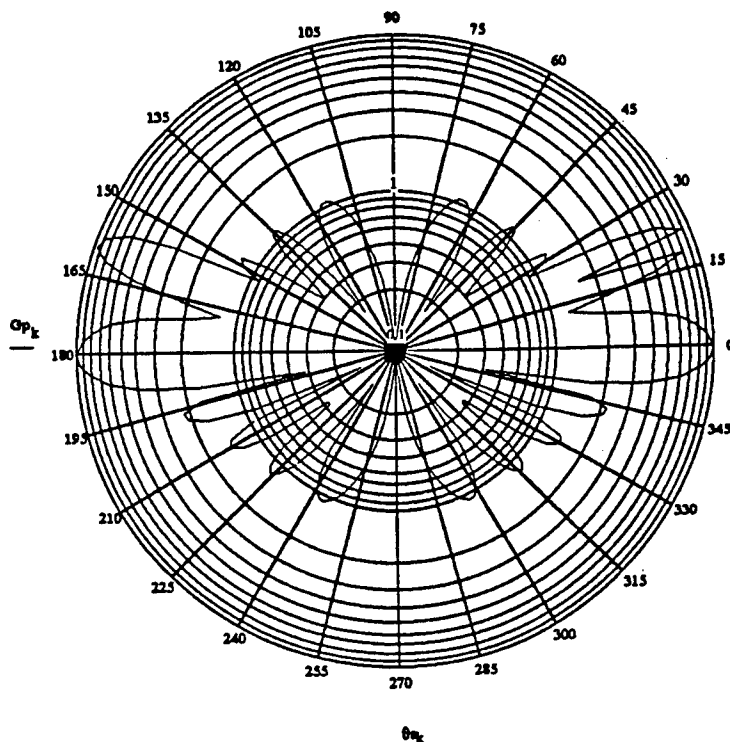
TABLE 1

<u>Element No.</u>	<u>TTD BF</u>	$f_n$ (MHz)	<u>Photonic BF</u>
1	$4.38 \times 10^6$		$4.35 \times 10^6$
2	1,709.9		1,657.1
3	1,067.7		1,084.7
4	575.7		551.7
5	440.8		420.9
6	430.3		434.3
7	290.7		291.7
8	260.6		261.2
9	270.9		269.7
10	195.6		192.9

TABLE 2

<u>Element No.</u>	<u>TTD BF</u>	$a_n$	<u>Photonic BF</u>
1	1.94		2.03
2	0.71		1.25
3	2.40		2.49
4	2.00		2.38
5	0.65		1.10
6	2.36		2.43
7	2.07		2.02
8	0.60		0.59
9	2.32		2.27
10	2.13		2.26

(a)



(b)

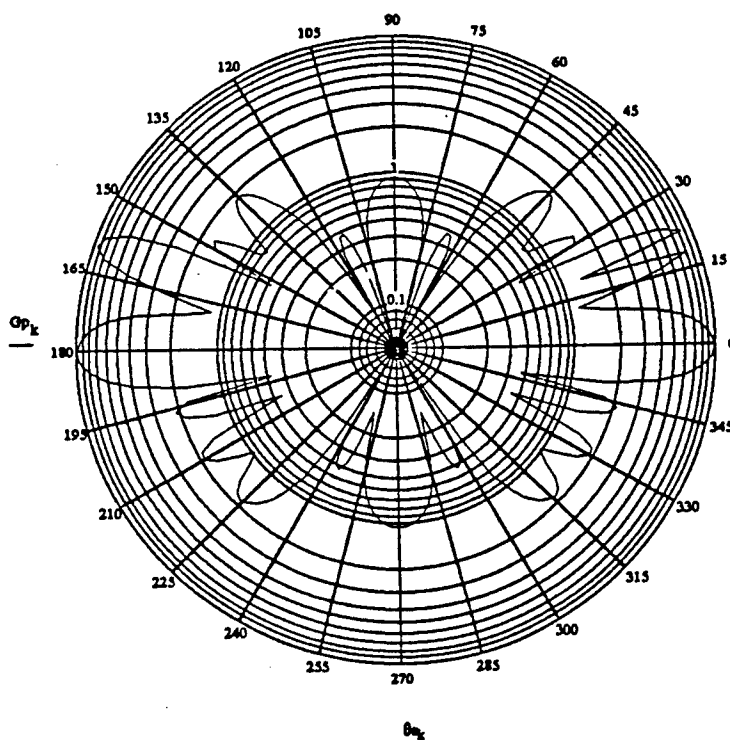
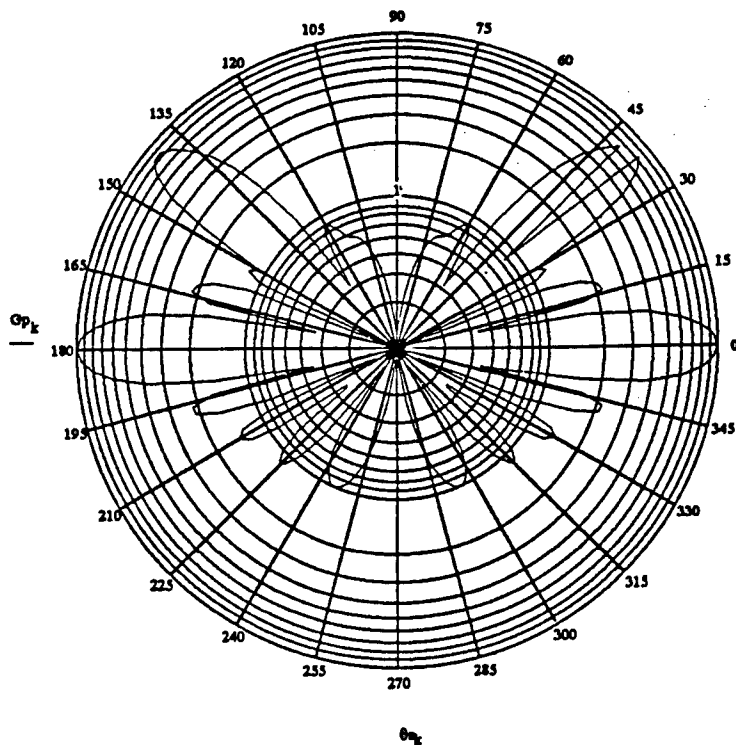


Figure 2: (a) Beampattern of an adaptive true time delay (TTD) beamformer for a 10-element line array, steered to  $0^\circ$ , with "jammer" at  $20^\circ$  and null steered to  $20^\circ$ ; (b) Beampattern of an adaptive photonic beamformer for a 10-element line array, steered to  $0^\circ$ , with "jammer" at  $20^\circ$  and null steered to  $20^\circ$ .

(a)



(b)

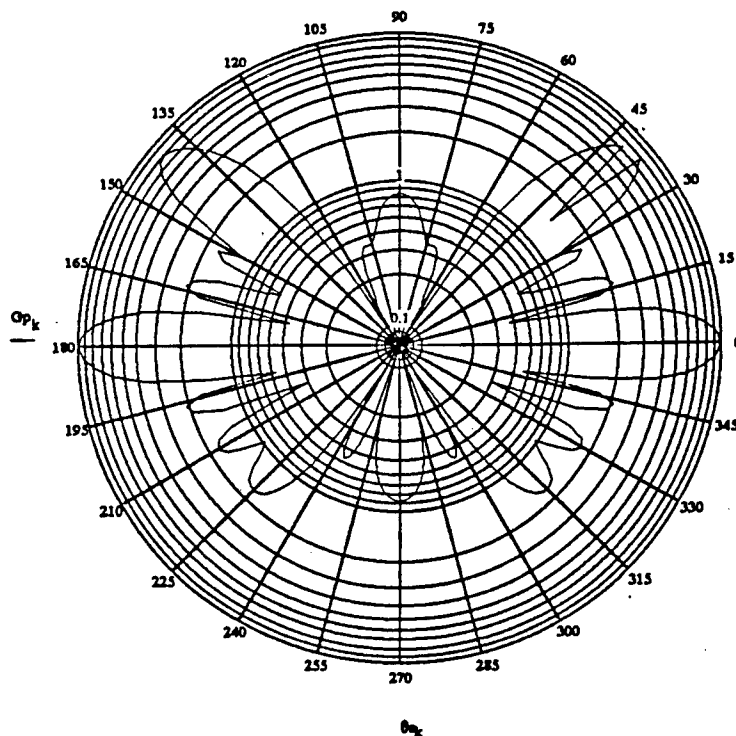


Figure 3: (a) Beampattern of an adaptive true time delay (TTD) beamformer for a 10-element line array, steered to  $0^\circ$ , with "jammer" at  $40^\circ$  and null steered to  $40^\circ$ ; (b) Beampattern of an adaptive photonic beamformer for a 10-element line array, steered to  $0^\circ$ , with "jammer" at  $40^\circ$  and null steered to  $40^\circ$ .



Their relative amplitudes, also obtained from the prescription of Section 3, especially Equation (12) are presented in Table 2.

## 5. DISCUSSION - TRANSMIT MODE

The results given above are both reassuring and troublesome. They are reassuring foremost because the photonic beamformer's performance is comparable to that of a TTD beamformer, *at least in theory*. The required implementation to reach this desirable goal is, however, seen to bring in several new concerns.

First, the introduction of multiple signals - multiple single-frequency waves, or modulations of a carrier - introduces a problem common to most communications systems based on AOMs: the potential for intermodulation effects. These effects are not considered here, but most likely deserve serious consideration.

Second, the specifications on the AOM change when adaptive beamforming is considered. As indicated in Table 1, a dynamic range running across frequencies as low as about 200 MHz and as high as 1.7 GHz (ignoring the unattainable  $4 \times 10^6$  MHz frequencies) is required.

Last, the ability to steer the individual tilting mirrors for each element becomes even more challenging, as the very different frequencies involved in the acousto-optic effect demand very different angular orientations to be captured.

Understanding how to do adaptive photonic beamforming is still in its early stages. The problems described briefly above have not been dealt with in a serious manner - yet. However, many encouraging results have been found, and a potentially useful method of carrying out adaptive null steering for a transmit array has been suggested.

## 6. INTRODUCTION - RECEIVE MODE

As pointed out by Toughlian and Zmuda [15], the photonic TTD beamformer is not readily reconfigured as a radar receiver due to the nonreciprocal nature of the AOM. In the receive mode of a beamformer, each incoming RF signal must be time delayed with a whole series of possible delays, and then all such delayed signals summed across the RF array elements. The correct choice of time delays is evidenced by a peak in the summed output for a particular set of delays. This operation will require a separate AOM to provide the set of potential delays for each RF element. Hence, a whole array of AOMs is required.

This undesirable hardware proliferation was addressed conventionally by Toughlian and Zmuda in Reference [15]. They used a set of optical fibers of differential lengths to provide the set of time delays. What was unconventional about the design of Reference [15] was the switching mode which allowed all possible sets of delays to be tried. Conventional switching between fiber delay lines has been electro-optic, which, as pointed out by Toughlian and Zmuda, is a power-hungry, high-loss, inefficient method. These authors suggest the use of a segmented mirror device (SMD) to shift the whole collection of individual RF element outputs along the fiber delays, arranged in an optically-addressed array. This configuration also allows for easy frequency agility and true time delay beamforming, since the appropriate set of linear time delays is obtained for a given frequency with just a new tilt angle of the SMD. This device will be described briefly in Section 7.

What was not accomplished in Reference [15] was a specific scheme for an adaptive receiver design. Before the specific capabilities of the Toughlian/Zmuda receiver are discussed, it would be beneficial to catalog and describe the evolution of the beamformer concept (staying with the one-dimensional line array for simplicity) from its simplest form to its most complex. In this way, the particular capabilities of each stage can be related to the underlying beamforming equation and to the photonic components or units required to realize the equation.

The "zero-th" stage of the beamformer would be a single, omnidirectional sensor. Modulo a constant, its output,  $s(t)$ , would equal its input,  $x(t)$ , and it would have no capability to discriminate between signals on the basis of their direction of arrival (bearing) or spectrum.

The simplest real beamformer would be a linear arrangement of a number of omnidirectional sensors (elements), separated from each other by a fixed distance  $d$  taken, for convenience, so that  $d = \lambda/2$  for the design signal wavelength  $\lambda$ . This beamformer could form a relatively narrow beam along its boresight direction, with sidelobes of reduced - but not necessarily

negligible - sensitivity off boresight. It would operate as expected only for the design wavelength and frequency. Any signal with a wavelength other than  $\lambda$  would suffer from "beam squint", a rotation of the peak sensitivity off of boresight. This beamformer's output would be a simple sum or integration:

$$s(t) = C \sum x_i(t); \quad s(t) = C \int_0^L x(t) dx \quad (15)$$

If one wants to steer the mainbeam off of boresight for a specific frequency (narrowband operation), the next stage of complexity to add to the beamformer is a delay  $(n-1)\delta$  to each element  $n$  along the linear array. Then  $c(n-1)\delta/d$  provides a fixed phase shift to the input of the  $n$ -th element. The output of the array is given by

$$s(t) = C \int_0^L x(t) \rho_x(x) dx \quad (16)$$

where  $\rho_x(x)$  represents the phase shift (a spatial weight) that produces the spatial steering.

Suppose one wanted to be able to adaptively steer the beam generated by the narrowband beamformer of Equation (16). It would be necessary to provide variable weights multiplying each element's output. The variable weights are produced by a reference function,  $r(t-x/v)$ , which are sets of delays required for the desired look directions. (Alternatively,  $r(t-x/v)$  could allow for broadband operation at a fixed bearing, as in the true time delay transmit beamformer.) The output of this spatially adaptive array for narrowband signals is given by

$$s(t) = C \int_0^L x(t) r(t-\frac{x}{v}) \rho_x dx \quad (17)$$

Note that  $x(t)r(t-x/v)$  is a convolution, readily realized through the use of photonic components [20]. For an automatically adaptive beamformer of this sort, the output  $s(t)$  would be compared to (actually, subtracted from) the "desired response" (signal only at the look direction, zero elsewhere), generating an error signal which would update the variable weights.

So far, it has not been possible to operate the spatially adaptive array for broadband signals and noise. In order to do so, each element must be given its own tapped delay line, similar in character to the original line array as a spatial tapped delay line. A time-delay function  $\rho_\tau(t-\tau)$  multiplying  $x(\tau)$  replaces  $x(t)$  in Equation (17), so that the output of the broadband spatially adaptive beamformer is

$$s(t) = C \int_0^L \left[ \int_{-\infty}^t x(\tau) \rho_r(t-\tau) d\tau \right] r(t-\frac{x}{v}) \rho_x(x) dx \quad (18)$$

Finally, a filtering operation with respect to frequency can be implemented by adding variable weights along each line of the elements' tapped delay lines. This is accomplished by inserting the reference function  $r^*(\tau-x/v)$ , which essentially selects where we "listen" in frequency, to the time integral. The output of the spatial/spectral adaptive beamformer is

$$s(t) = C \int_0^L \left[ \int_{-\infty}^t x(\tau) r^*(\tau-\frac{x}{v}) \rho_r(t-\tau) d\tau \right] r(t-\frac{x}{v}) \rho_x dx \quad (19)$$

Notice that the product  $x(\tau)r^*(\tau-x/v)$  is a correlation, and is easily realized by photonic components [20]. The correlation is equivalent to a matched filter for the spectral characteristics of the reference. A convolution of the result of the correlation operation with the factor  $\rho_r(t-\tau)$  completes the integrand. Note that the integrand of the time integral is a triple-product processor, also readily produced by a pair of AOMs in a crossed configuration [21]. Again, for real-time adaptivity, it is necessary to use this output, subtracted from a desired response, to generate an error signal which is then used to adjust the weights for each delay line of each element.

After an introduction to the Toughlian/Zmuda receiver design, that design, as well as several others, will be compared to the beamformer stages of evolution described above.

## 7. CONFIGURATION FOR A BROADBAND RECEIVER

Figure 4 is a schematic for the broadband TTD photonic receiver of Reference [15], for one RF element's input in particular. The RF signal is shown as modulating the output of a laser via an electro-optic (EO) modulator. For an entire array of RF elements (see Figure 5), a separate EO modulator (though not necessarily a separate laser, since the optical output can be split) would be required for each radar element. Alternatively, one could drive a separate laser diode with each phased array element's RF signal, directly modulating its output.

The modulated optical signals derived from all the radar elements are brought together in an array of GRINrod lenses. The

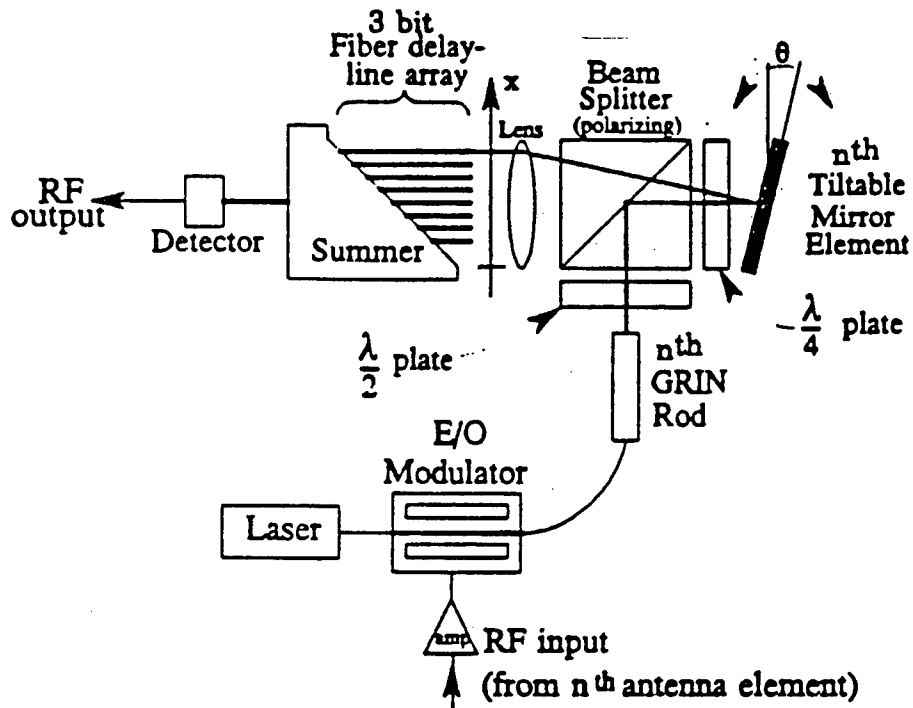


Figure 4: Single quantized variable delay line and experimental setup [15].

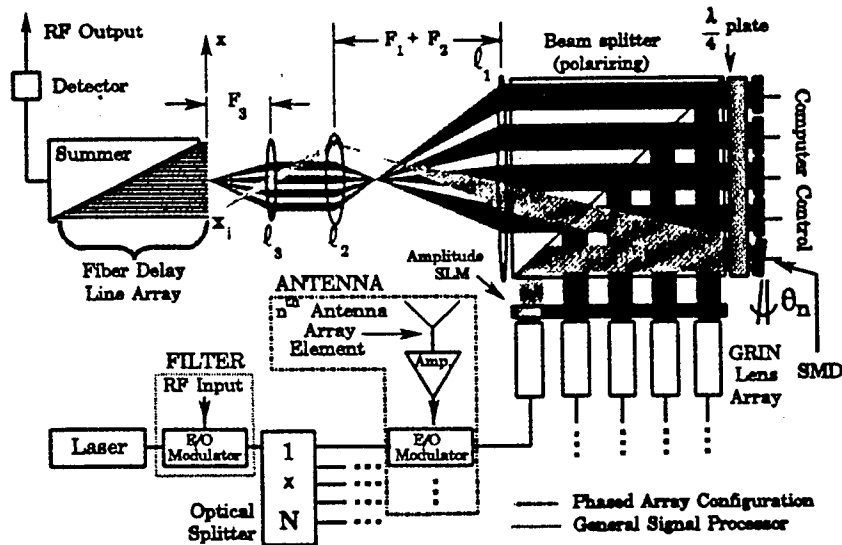


Figure 5: Schematic diagram of the full Toughlian/Zmuda phased array receiver.

light from each lens (and, hence, from each microwave element) is directed by a single polarized beamsplitter to a unique location on the surface of the SMD. (Optical polarization is manipulated in order to keep stray, unwanted beams out of the picture.) At the SMD, a separate tiltable mirror element can direct that particular optical ray to whatever location is desired along the optical fiber array, thereby providing the optical signal with its own unique time delay. For simple beamforming, the mirror elements will all have the same tilt, which will vary as the center frequency of the RF signal changes, to keep the direction of the beam formed fixed (the TTD aspect); for special applications, such as null cancelling, the tilts will not be uniform.

After each optical signal (each representing a different element in the radar array) has been time delayed as required for a particular beam direction, the optical outputs are summed; this is the same summation as that indicated in Equation (1). For that choice of direction, ie, that particular choice of element time delays, at which an RF signal does exist, the summation will result in a large output. If no RF signal exists along a particular direction, then the summation of time delayed optical signals will be a minimum, ideally zero.

## 8. ADAPTIVE CONFIGURATIONS OF THE PHOTONIC RECEIVER

### A. CONFIGURATION USING THE SMD

The optical fiber array essentially provides quantized weights to the RF element signals which are fixed in their relative phases. However, the SMD provides the freedom to direct each RF element's signal separately to a different location along the fiber optic array. Hence, each individual RF signal can be given its own required phase weighting. Amplitude weighting is a bit trickier, but may, perhaps, be handled by using two delay lines [2]. For an open-loop adaptive process, like the cancelling of a known noise source in a given direction, all that needs to be done is to pre-calculate the appropriate phase shift (time delay) for each element and direct its particular element of the SMD for the tilt angle required to place that light ray at its appropriate optical fiber. This process results in a beamformer of the type given by Equation (17). It can be considered a wideband beamformer if the single factor  $r(t-x/v)$  is used as a true time delay line. Alternatively, the beamformer could be viewed as a narrowband, spatially adaptive array. If the "RF Output" (see Figure 5) of the beamformer were subtracted from a desired response function, the resulting error could be fed back to the system weights (probably at the SMD) and would produce an automatic narrowband, spatially adaptive array.

For such closed-loop adaptive beamforming, eg, forming nulls as required to cancel noise sources as they arise, feedback must

be provided to the elements of the SMD. In particular, the RF output shown in Figure 4 must be electronically analyzed and new weights calculated for each RF element, implying a new tilt angle for each element of the SMD. The calculation of the weights (phase and amplitude) needed is well known (see again References [9-11]). The performance of the required calculations using typical, sequential digital electronic processors is not a totally desirable feature, since these calculations require massive commitments of computational power, and still may be comparatively slow, even with current processors. However, several methods of performing the adaptive beamforming calculations *photonicall*y are known. (See, for example, References [16-19].) In the next Section, several methods are reviewed which combine spatial and spectral adaptive filtering in a photonic beamformer, producing the fully evolved beamformer of Equation (19) (operated in closed-loop mode). In Section 8.C., a suggestion is made as to how to marry these photonic adaptive filtering techniques with the frequency agility of the Toughlian/Zmuda photonic beamformer.

#### B. TOTALLY PHOTONIC CONFIGURATIONS OF A FULLY ADAPTIVE BEAMFORMER

Figure 6 displays a closed-loop, spatially adaptive, spectral filtering beamformer of the type described by Equation (19) due to Psaltis and Hong [16]. The top part of the diagram is a two-dimensional acousto-optic convolver and photodetection, representing the space-variable integrand and integration, respectively. The bottom part of the diagram carries out the time-variable triple product, and is a combination of the correlation (matched filtering) - the left side of the optical layout - and multiplication by the time-dependent weights - the inclusion of the right-side part of the layout. Psaltis' and Hong's "steering vector" has been called the "desired response" in this paper. The error signal, used to automatically adapt the weights, is indicated by  $h(t)$ , and results from the subtraction of the beamformer output from the desired response, as required.

Figures 7a and 7b are VanderLugt's realizations of an adaptive filter for a communications-type single received signal. Only the time-integral part of Equation (19) is relevant to this design. A phased array beamformer could incorporate this acousto-optic triple-product processor for each element of the array and create a fully spatially and spectrally adaptive beamformer. Figure 7a represents the correlation of the input signal with a "residual signal", the latter being equivalent to the error signal referred to in Section 6, incorporated directly into the triple-product processor by adapting the "reference function" of Section 6. The correlation results in an array of tap weights which are then convolved with the time-delay factors (Section 6:  $\rho_r(t-\tau)$ ), as indicated in Figure 7b. If the combined system of Figures 7a and 7b is incorporated into one arm of an

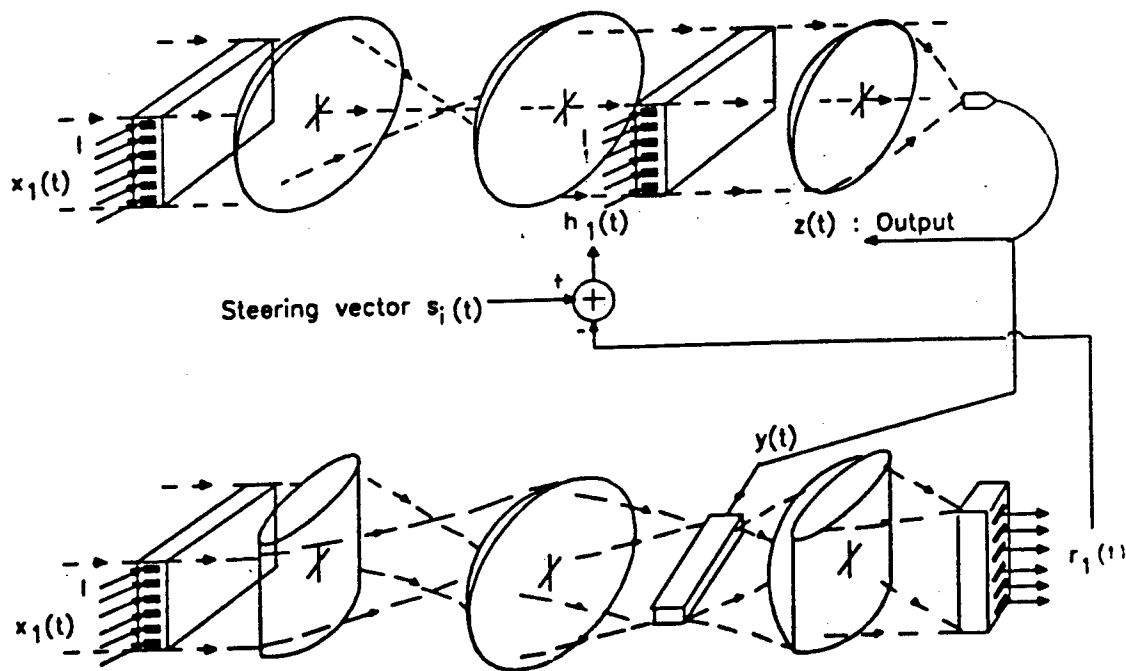


Figure 6: Fully adaptive - spatially and spectrally - photonic receiver system [16].

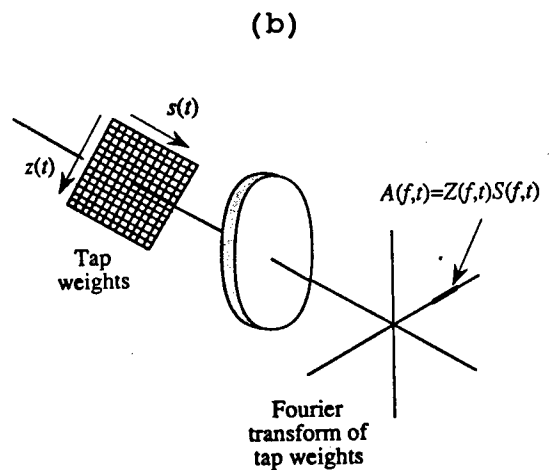
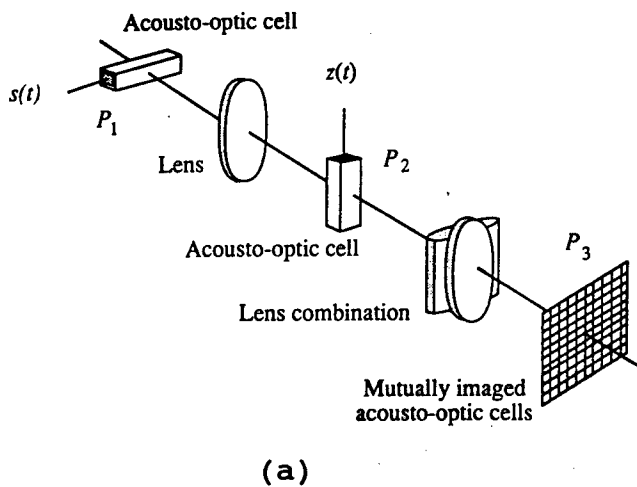


Figure 7: (a) Acousto-optic cell system for producing tap weights [21]; (b) Optical system to produce Fourier transform of tap weights [21].



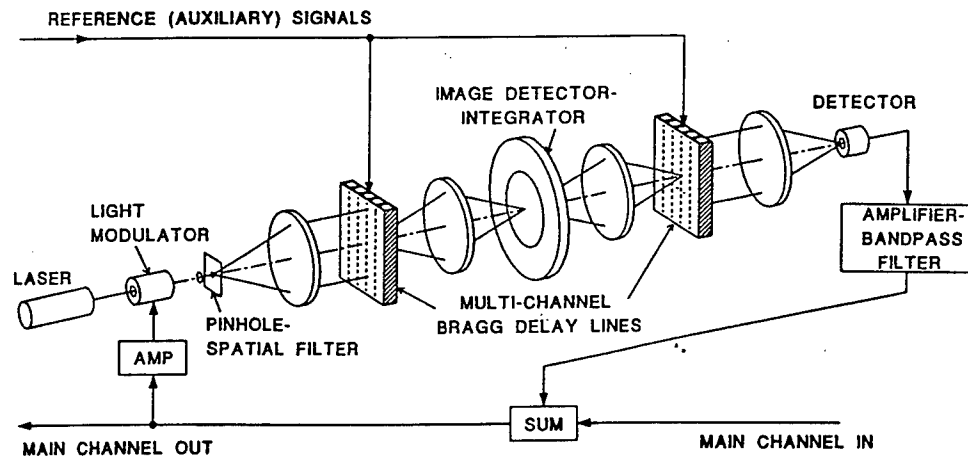


Figure 8: Penn's adaptive interference canceller using time and space integrating correlators [22].

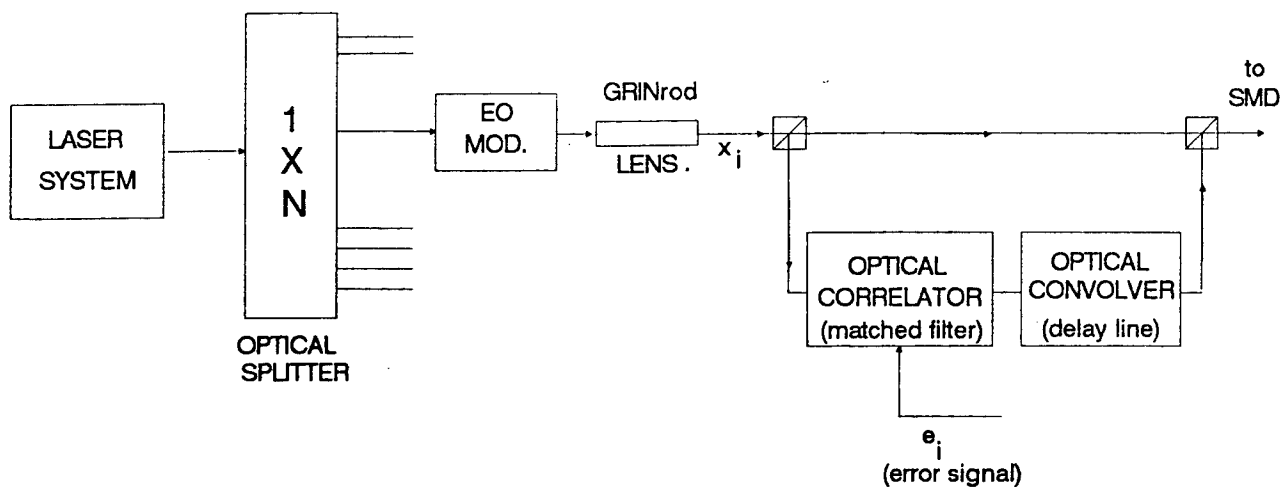


Figure 9: Schematic diagram of a fully adaptive photonic receive beamformer.

interferometer, the recombined interferometric signal can be detected by a single photodiode and then provides the estimate of the input signal.

Finally, Figure 8 shows a realization of the fully spatially and spectrally adaptive beamformer due to William Penn [22]. The interference-cancelled (see SUM block) radar signal amplitude modulates a laser whose output is directed through a multichannel AOM which is RF-driven by the reference function. The result, imaged onto the "Image Detector-Integrator", is the set of tap weights due to the correlation part of the triple-product processor. The final multichannel AOM carries out the required convolution function.

### C. A FULLY ADAPTIVE EXTENSION OF THE TOUGHLIAN/ZMUDA RECEIVE BEAMFORMER

As indicated above, several investigators have produced photonic configurations, based on multiple AOMs, or AOMs in combination with photorefractive devices or electronic memories, for narrowband adaptive beamforming. It is suggested in this Section that a marriage can take place between the excellent broadband/frequency-agile capabilities of a Toughlian/Zmuda type TTD photonic beamformer and the already established possibilities for AOM-based adaptive receiver functions.

A schematic of the proposed broadband/frequency agile adaptive receiver is provided in Figure 9. The input of each radar element's signal via a modulated light ray in a GRINrod lens assembly is the same as that of Figure 4. The polarizing optics and polarized beamsplitter are also retained. The SMD will provide the spatial adaptivity (thereby moving to a narrowband configuration if no more is done), but the spectral adaptivity part will be provided by a configuration of AOMs and, possibly, other spatial light modulators which realize the triple-product processor part of Equation (19).

Then a photonic adaptive processor, such as that suggested in Reference [21] and pictured in Figure 7, can be used to perform the appropriate calculations for adaptive receiving in the chosen frequency range. The receiver pictured in Figure 7 is, as previously discussed, a combination of two, fundamental optical processors: a convolver, and a correlator, producing an optical triple product.

## 9. DISCUSSION - RECEIVE MODE

The Toughlian/Zmuda receive mode photonic beamformer (Ref. [15]) can be viewed as either a broadband phased array receiver, or a spatially-adaptive narrowband receiver; it was conceived as

the former. In order to produce a fully spatially and spectrally adaptive beamformer from the Toughlian/Zmuda model, each element must be given a tapped delay line of its own, with adjustable weights. This is equivalent to incorporating a triple-product processor - potentially, photonic - for each element. A simple means of doing so has been suggested here, with several different realizations of the triple-product processor itself available from among examples discussed in Section 8.B.

There are choices to be made which all impact the size, weight, and stability of the final beamformer. Toughlian and Zmuda have expressed [15] a desire to avoid the cumbersome necessity of multiple AOMs, however, multiple crossed AOMs is the realization suggested by VanderLugt [21]. His tap weights, appearing as if suspended in mid-air in Figure 7, must be saved somewhere. Penn [22] suggests that, in fact, the delay times of the AOMs provide the storage needed in VanderLugt's case. Penn himself uses an image detection device - a liquid crystal light valve (LCLV) - in this role. He suggests a photorefractive device as another alternative. Both devices have some problems: the LCLV dynamical range constraints and an asymmetry in response for falling versus rising light levels. The photorefractive devices require extreme attention to random background noise levels. Use of AOMs as in VanderLugt's design depends on the time-bandwidth products of the modulators relative to storage considerations. Psaltis' and Hong's device [16] is most like VanderLugt's, in this regard. It may be possible to implement a collection of SMDs for the required triple products, although this avenue may itself become the more cumbersome approach when each element must be outfitted with such a device.

## 10. REFERENCES

1. Toughlian, E.N. and Zmuda, H., "A Photonic Variable RF Delay Line for Phased Array Antennas", J. Lightwave Technol., vol. 8, no. 12, pp.1824-1828, 1990.
2. Zmuda, H. and Toughlian, E.N., "Adaptive Microwave Signal Processing: A Photonic Solution", Microwave Journal, vol. 35, no. 2, 1992.
3. Monsay, Evelyn H., "Photonic Delay Line for High-Frequency Radar Systems", Final Report, Air Force Office of Scientific Research Summer Faculty Research Program, August 1992.
4. Monsay, Evelyn H. and Lt. Michael Caccuitto, "Photonic Delay Line for High-Frequency Phased Array Systems", presented at PSAA-III Conference, January 1993.
5. Monsay, Evelyn H., "Form and Implications of the Nonlinear Dependence of Phase on Frequency for an Acousto-Optic Beamformer", Final Report, Air Force Office of Scientific Research Summer Faculty Research Program, August 1993.
6. Monsay, E. H., Baldwin, K. C., and Caccuitto, M. J., "Photonic True Time Delay for High-Frequency Phased Array Systems", IEEE Phot. Tech. Lett. Vol. 6, No. 1, January 1994, pgs. 118-120.
7. Monsay, Evelyn H., "Systems Analysis for a Photonic Delay Line", Final Report, Air Force Office of Scientific Research, Research Initiation Program, March 1994.
8. Monsay, Evelyn H., "Demonstration and analysis of a frequency-agile photonic beamformer", SPIE Conference Proceedings No. 2216, "Photonics at the Air Force Photonics Center", eds. Andrew R. Pirich and Paul Sierak, 4-5 April 1994, pgs. 130-141.
9. Sidney P. Applebaum, "Adaptive Arrays", IEEE Trans. Antennas and Propag. **AP-24**:585-598 (1976).
10. B. Widrow, P.E. Mantey, L.J. Griffiths, and B.B. Goode, "Adaptive Antenna Systems", Proc. IEEE, Vol. 55, No. 12, December 1967, pgs. 2143-2159.
11. Owsley, Norman L., "Modern Space-Time Signal Processing", Course Notes, Applied Technology Institute, Clarksville, MD, 1993.
12. Mailloux, Robert J., Phased Array Antenna Handbook, Artech House, Norwood, MA, 1994.

13. Monsay, Evelyn H., "Systems Analyses and Applications for a Photonic Delay Line", Final Report, Photonics Center, Rome Laboratory, Griffiss AFB, NY, January 1995.
14. Monsay, Evelyn H., "Calculation of System-Level Performance Parameters for a Photonic Beamformer", presented at PSAA-V Conference, January 1995.
15. Toughlian, E.N. and Zmuda, H., "Variable time-delay system for broadband phased array and other transversal filtering applications", Opt. Eng., Vol. 32, No. 3, March 1993, pgs. 613-617.
16. Psaltis, D. and Hong, J., "Adaptive Acoustooptic Processor", Proc. SPIE, Vol. 519, 1984, pgs. 62-68.
17. Vander Lugt, A., "Optical transversal processor for notch filtering", Opt. Eng., Vol. 23, No. 3, May/June 1984, pgs. 312-318.
18. Rhodes, Joanne F., "Adaptive filter with a time-domain implementation using correlation cancellation loops", Appl. Optics, Vol. 22, No. 2, January 15, 1983, pgs. 282-287.
19. Riza, Nabeel A. and Psaltis, Demetri, "Acousto-optic signal processors for transmission and reception of phased-array antenna signals", Appl. Optics, Vol. 30, No. 23, August 10, 1991, pgs. 3294-3303.
20. Rhodes, William T., "Acousto-Optic Signal Processing: Convolution and Correlation", Proc. IEEE, Vol. 69, No. 1, January 1981, pgs. 65-79.
21. VanderLugt, Anthony, Optical Signal Processing, John Wiley & Sons, New York, NY, 1992.
22. Zmuda, Henry and Toughlian, Edward N., Photonic Aspects of Modern Radar, Artech House, Boston, MA, 1994.

## ***MISSION OF ROME LABORATORY***

Mission. The mission of Rome Laboratory is to advance the science and technologies of command, control, communications and intelligence and to transition them into systems to meet customer needs. To achieve this, Rome Lab:

- a. Conducts vigorous research, development and test programs in all applicable technologies;
- b. Transitions technology to current and future systems to improve operational capability, readiness, and supportability;
- c. Provides a full range of technical support to Air Force Material Command product centers and other Air Force organizations;
- d. Promotes transfer of technology to the private sector;
- e. Maintains leading edge technological expertise in the areas of surveillance, communications, command and control, intelligence, reliability science, electro-magnetic technology, photonics, signal processing, and computational science.

The thrust areas of technical competence include: Surveillance, Communications, Command and Control, Intelligence, Signal Processing, Computer Science and Technology, Electromagnetic Technology, Photonics and Reliability Sciences.